

OSA 2024

Employing Frequency-Modulated Signals for Tonal Excitation in Airborne Sound Insulation Measurements

Dominik MLECZKO[Ⓜ], Marcjanna CZAPLA*[Ⓜ], Tadeusz WSZOŁEK[Ⓜ],
Wojciech KOTALA, Jadwiga HYLA, Dominika MUZYK,
Wiktoria POTONIEC, Jan BIŃKOWSKI, Maciej POSŁUSZNY,
Aleksandra SAWCZUK

*AGH University of Krakow, Faculty of Mechanical Engineering and Robotics
Department of Mechanics and Vibroacoustics*

Krakow, Poland;

e-mails: dmleczo@agh.edu.pl, twszolek@agh.edu.pl, kotala@student.agh.edu.pl,
hylajadwiga@student.agh.edu.pl, dmuzyk@student.agh.edu.pl,
wpotoniec@student.agh.edu.pl, janbinkowski@student.agh.edu.pl,
nieposluszny@student.agh.edu.pl, asawczuk@student.agh.edu.pl

*Corresponding Author e-mail: mczapla@agh.edu.pl

To enhance the similarity of acoustic insulation testing conditions in the laboratory, a tonal signal was employed as the excitation signal, reflecting real-world scenarios, such as transformer noise. To mitigate the non-uniformity of the acoustic field associated with tonal excitation, a tonal excitation with frequency modulation (FM) was applied in the experiment.

An experimental verification was first conducted to assess the influence of modulated signal parameters – modulation depth and frequency – on improving the uniformity of sound pressure distribution and reverberation time. Subsequently, acoustic insulation measurements were taken in a set of reverberation chambers using tonal excitation with the experimentally optimized FM modulation parameters. The results were compared with data obtained from measurements using noise excitation and harmonic excitation without modulation.

Preliminary findings indicate that FM signals significantly reduce the non-uniformity of the acoustic field in both chambers compared to tonal signal, as well as the reverberation time in the receiving chamber. Consequently, the quality of acoustic insulation measurements improved with reduced result variability and increased “fidelity” to real-world conditions.

Keywords: sound insulation; reverberation time; frequency-modulated signal; tonal signal; measurement uncertainty; reverberation chamber.



1. INTRODUCTION

Airborne sound insulation is typically measured using a broadband excitation signal [1], such as noise or impulsive excitation generated by the swept-sine method or maximum length sequence (MLS) method [2]. However, to better replicate real-world conditions, excitation signals that closely resemble these conditions may be employed. These signals could be either original signal recordings from real environments or artificially generated. Such situations might arise when analyzing methods to reduce tonal noise generated by transformers, pumps, or fans. This is particularly important for transformers, which are characterized by tonal sound (with a frequency of 100 Hz and its higher harmonics). The 100 Hz frequency corresponds to twice the power frequency. To better approximate the results of acoustic insulation measurements conducted in laboratory conditions (using noise excitation) to real-world conditions, tonal excitation was applied during the acoustic insulation measurements.

However tonal excitation is associated with the problem of standing waves forming in the reverberation chamber. This leads to significant non-uniformity in the acoustic field [3]. This, in turn, causes substantial errors in determining the sound power incident on and radiated by the sample. To address the adverse effects of standing waves associated with tonal excitation, a frequency-modulated signal can be applied [4, 5], similar to the approach used in reverberation time measurements. The study employed cyclic frequency modulation of the tonal excitation signal, corresponding to frequency modulation (FM).

2. LABORATORY TESTS

2.1. *Measurement setup*

The sound insulation measurements were conducted at the laboratory of the Department of Mechanics and Vibroacoustics at the AGH University of Science and Technology in Kraków, utilizing a test setup designed for acoustic insulation assessment. The laboratory featured two reverberation chambers: a source room with a volume of 178.77 m³ and a receiving room with a volume of 176.9 m³. A measurement aperture measuring 1 × 2 m was positioned between the two chambers. For evaluating smaller samples with dimensions of 0.7 × 0.84 m, an additional barrier was placed within the measurement window.

The measurement setup (Fig. 1) comprised two Norsonic 1/2" Type 1220 pressure microphones, a JBL speaker, a Sound KRAK power amplifier, a Norsonic 850 analyzer, and a PC equipped with data acquisition software and a digital audio workstation for generating tonal and modulated excitation signals. A loudspeaker (sound source) in receiving room was used to determine reverberation time and to calculate the room's acoustic absorption A (Eq. (2.2)).

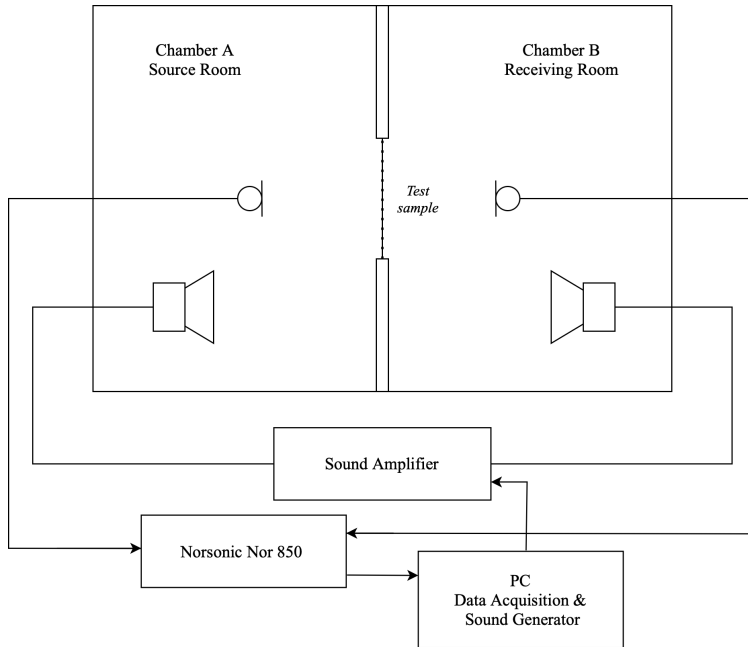


FIG. 1. Measurement base diagram.

2.2. Test method

The airborne sound insulation of the tested sample is determined according to the following formula:

$$(2.1) \quad R = L_1 - L_2 + 10 \log \left(\frac{S}{A} \right), \text{ dB},$$

where L_1 is the averaged sound pressure level in the source room and L_2 is the averaged sound pressure level in the receiving room. The sound pressure levels are expressed in decibels (dB). The surface area S of the test sample, in square meters, corresponds to the area fully occupied by the mounted sample. The acoustic absorption A is calculated using the following equation:

$$(2.2) \quad A = \frac{0.16V}{T},$$

where V is the volume of the receiving room in cubic meters and T is the reverberation time in seconds.

The reverberation time values required for the calculation of acoustic insulation, as shown in Eq. (2.2), were obtained by positioning a sound source within the receiving chamber (Fig. 1). Measurements were conducted at the

same spatial points used for determining the sound pressure levels. The measurements were performed by introducing the test signal for a duration of 10 s to achieve acoustic saturation of the room. Subsequently, the decay of the sound field was recorded over a 20-second interval, from which the reverberation time parameter T_{20} was calculated.

The average sound pressure levels L_1 and L_2 were determined based on measurements taken at multiple measurement points. A microphone mounted on a movable, controllable arm with a 1.4 m radius was used, while the sound source was positioned in two different locations. To ensure accurate and repeatable measurements, the location of each point was programmed into the actuator controller, allowing precise reproduction of the same positions during subsequent measurements. The measurement points were distributed at three heights: 1.5 m, 1.8 m, and 2.0 m, with 32 points evenly distributed along a circle at each height (Fig. 2). In total, measurements were taken at 96 points for each sound source position.

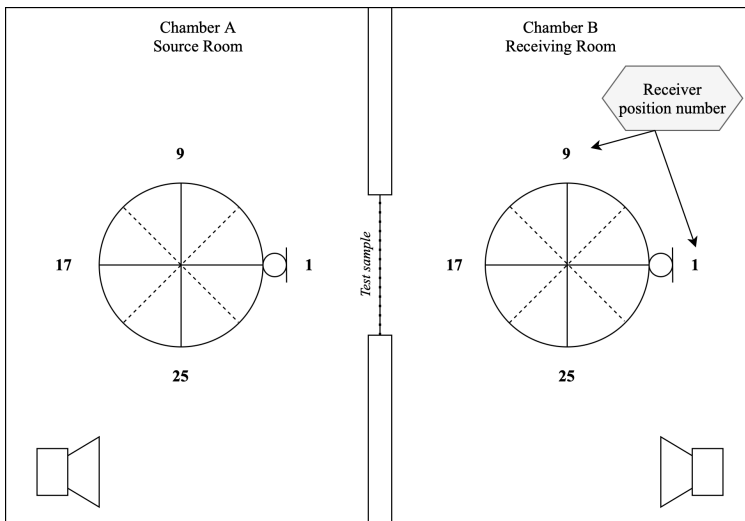


FIG. 2. Orientation of measurement points in test rooms.

This study examined the efficacy of frequency modulation in acoustic insulation measurements, using two rectangular samples measuring $0.7 \text{ m} \times 0.84 \text{ m}$. The sample dimensions were constrained to these specified sizes due to the limitations of the mounting surface available in the laboratory where the measurements were conducted. The samples included a homogeneous 6 mm thick plexiglass plate and a laminated two-layer sample consisting of a 1 mm thick steel plate and a 3 mm thick rubber layer.

2.3. Test signals

In the conducted acoustic measurements, sinusoidal waveforms with frequencies of 100 Hz, 200 Hz, 300 Hz, and 500 Hz were initially used as the primary excitation signals. Subsequently, signals with the same frequencies but with FM were applied, where the modulation frequency was 5 Hz, and the modulation depth was 10% of the fundamental frequency. Pink noise excitation was used as a reference for comparison of the results.

2.4. Measurement uncertainty

To estimate measurement uncertainty, method A [6] was applied, focusing on the standard uncertainty that reflects the dispersion of measurement results. Other partial uncertainties, such as those contributed by the equipment and the physical parameters of the tested samples and reverberation chambers, remain constant and independent of the type of excitation used.

When the measurement result depends on several input parameters, the measurement uncertainty of the result is a function of the partial uncertainties of the input quantities, as shown below:

$$(2.3) \quad L_{out} = f(X_{in1} + X_{in2} + \dots + X_{inn}),$$

where each input element $X_{in(i)}$ carries a certain uncertainty. For uncorrelated results, the combined standard uncertainty can be determined using the following formula [7]:

$$(2.4) \quad u_c = \sqrt{\sum_{i=1}^n \left(\frac{\partial f}{\partial X_{in(i)}} \right)^2 u^2(X_{in(i)})},$$

where u_i is the partial uncertainty of the i -th input parameter of the function defined by the general relationship in Eq. (2.1). The partial uncertainties u_i of sound pressure levels and reverberation time are standard uncertainties. The expanded uncertainty U is obtained by multiplying the combined standard uncertainty u_c by an expansion factor k , as shown in the following equation:

$$(2.5) \quad U_{95} = k \cdot u_c,$$

where k is the coverage factor, typically chosen to provide a specific confidence level for the uncertainty estimate.

For a normal distribution of measurement errors, the coverage factor is 2, which corresponds to a confidence level of 95%. In this study, the measurement uncertainty was calculated according to the above assumptions.

3. RESULTS AND ANALYSIS

3.1. Reverberation time

The results of reverberation time measurements using different excitation types (pink noise, sine wave, and modulated sine wave) are presented in Table 1. Reverberation time measurements for broadband noise were conducted using the interrupted noise method. Pink noise excitation produced the most stable results (with the smallest standard deviations) compared to the other types of excitations. The most dispersed results were recorded with tonal excitation (highest standard deviation), particularly noticeable in the 200 Hz frequency band, where the variability was twice as high, and in the 315 Hz frequency band, where it was more than three times greater than the variability observed with noise measurements, and twice as high as the variability obtained with modulated excitation. A similar spread was noted for tonal and FM excitation in the 100 Hz band.

TABLE 1. Reverberation time determined in the receiving chamber.

Type of excitation	Average reverberation time, s	Standard deviation, s	Max reverberation time, s	Min reverberation time, s
100 Hz				
Pink noise	9.3	0.6	11.1	7.9
Sine wave	10.0	0.9	11.9	6.8
FM sine wave	9.4	0.9	11.2	7.9
200 Hz				
Pink noise	8.0	0.5	9.7	6.5
Sine wave	7.8	1.1	16.1	4.7
FM sine wave	7.4	0.6	8.6	5.2
315 Hz				
Pink noise	7.3	0.5	8.7	6.2
Sine wave	6.8	1.7	11.5	2.7
FM Sine wave	7.9	1.0	10.2	5.2
500 Hz				
Pink noise	4.7	0.3	5.5	3.7
Sine wave	4.1	1.3	7.9	1.4
FM Sine wave	4.1	0.4	5.2	2.5

The average values of the measured reverberation times do not differ significantly and are fall within the standard deviation range of reverberation times measured using the interrupted noise method.

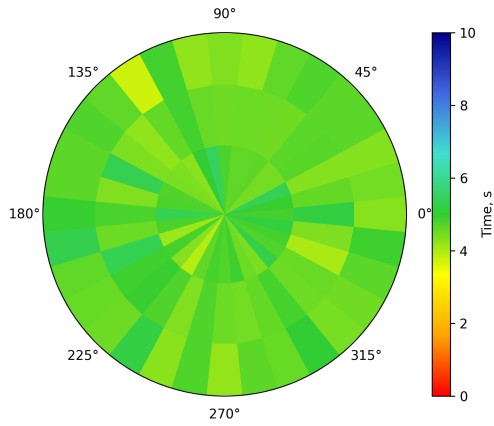


FIG. 3. Reverberation time (500 Hz), source position S1, pink noise.

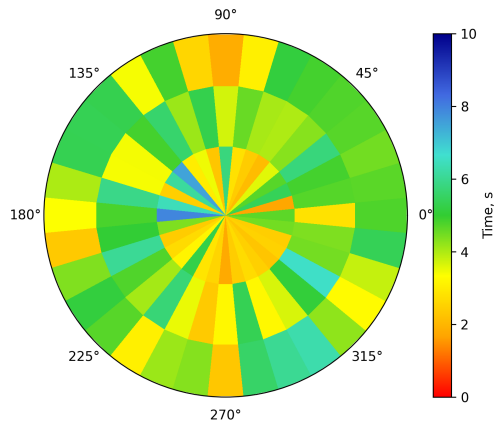


FIG. 4. Reverberation time (500 Hz), source position S1, sine wave 500 Hz.

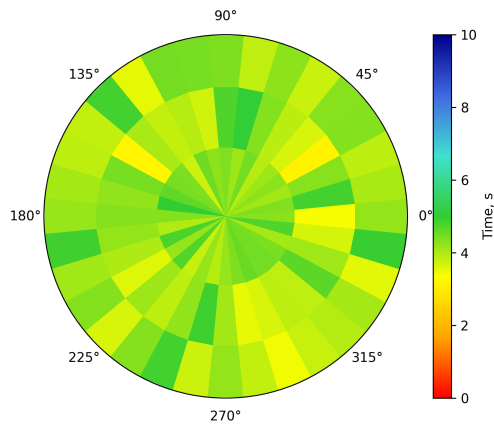


FIG. 5. Reverberation time (500 Hz), source position S1, FM sine wave 500 Hz.

The heat map provides an easy comparison of measurement result differences between pink noise (Fig. 3), tonal excitation (Fig. 4), and FM excitation (Fig. 5). This visualization helps to observe how each type of excitation affects the variability of reverberation time at different measurement points, and helps to identify areas with the highest and lowest data dispersion.

According to Eq. (2.2), the acoustic absorption of the receiving room was determined along with the standard uncertainty $u_c(A)$ (Table 2).

TABLE 2. Absorption A with standard uncertainty.

Type of excitation	Pink noise		Sine wave		FM Sine wave	
Results	Average, m^2	Uncertainty $u_c(A)$, m^2	Average, m^2	Uncertainty $u_c(A)$, m^2	Average, m^2	Uncertainty $u_c(A)$, m^2
100 Hz	9.3	0.6	10.0	0.9	9.4	0.9
200 Hz	8.0	0.5	7.8	1.1	7.4	0.6
315 Hz	7.3	0.5	6.8	1.7	7.9	1.0
500 Hz	4.7	0.3	4.1	1.3	4.1	0.4

3.2. Sound pressure level

The results of the sound pressure measurements for the homogeneous sample (Table 3) and the layered sample (Table 4), using all three types of excitations – broadband noise, tonal, and FM – are presented below in Tables 3 and 4.

TABLE 3. Sound pressure level in the source room L_1 and receiving room L_2 with standard uncertainty; homogeneous sample.

Type of excitation	Pink noise		Sine wave		FM sine wave	
Results	Average, dB	Uncertainty $u_c(L_i)$, dB	Average, dB	Average $u_c(L_i)$, dB	Average, dB	Uncertainty $u_c(L_i)$, dB
Sound pressure level in source room						
100 Hz	94.5	1.4	85.9	5.7	90.9	3.3
200 Hz	94.1	0.9	85.7	5.4	84.9	2.1
315 Hz	93.8	0.6	87.7	5.8	85.6	2.2
500 Hz	97.3	0.7	89.0	6.7	86.1	1.6
Sound pressure level in receiving room						
100 Hz	68.4	2.3	48.9	6.3	56.6	4.7
200 Hz	67.4	1.3	57.0	6.7	59.3	3.3
315 Hz	63.3	0.8	57.0	6.4	53.5	2.5
500 Hz	63.3	0.5	55.6	6.7	56.0	2.0

TABLE 4. Sound pressure level in the source room L_1 and receiving room L_2 with standard uncertainty; two-layer sample.

Type of excitation	Pink noise		Sine wave		FM sine wave	
Results	Average, dB	Uncertainty $u_c(L_i)$, dB	Average, dB	Average $u_c(L_i)$, dB	Average, dB	Uncertainty $u_c(L_i)$, dB
Sound pressure level in source room						
100 Hz	93.3	1.5	89.6	4.5	90.3	4.7
200 Hz	93.2	0.9	91.9	8.4	84.4	2.7
315 Hz	93.0	0.7	91.2	6.8	85.3	2.1
500 Hz	96.4	0.6	88.3	5.6	85.6	1.4
Sound pressure level in receiving room						
100 Hz	63.8	2.6	49.0	7.2	50.8	4.0
200 Hz	65.0	1.6	65.7	9.2	54.8	2.8
315 Hz	60.5	1.4	59.8	9.1	55.1	3.8
500 Hz	60.6	2.0	50.8	6.6	50.9	1.9

The smallest standard uncertainty in the measurement of sound pressure level was recorded with noise excitation, which typically provides more consistent and reliable measurements compared to the more variable tonal excitation. Furthermore, as expected, the uncertainty in sound pressure level measurements decreases with increasing frequency.

The illustrations below depict the visualization of sample distributions of the sound pressure level measured in both the source and receiving rooms for the homogeneous sample (Figs. 6–11) with one sound source position. The distribution results for the second sound source position, as well as for the measurement of the separate second sample, exhibit similar trends. Therefore, illustrations for

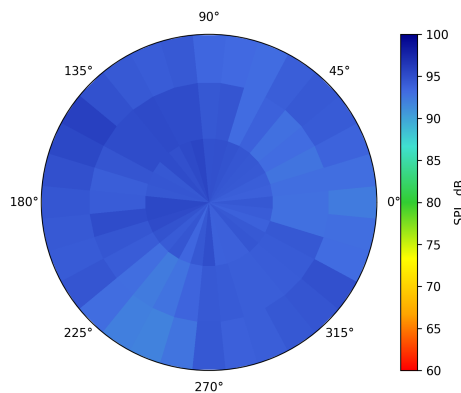


FIG. 6. Sound pressure level (200 Hz) in the source room, source position no. 1, pink noise; homogeneous sample.

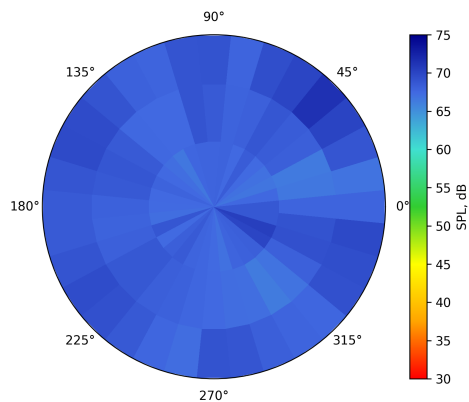


FIG. 7. Sound pressure level (200 Hz) in the receiving room, source position no. 1, pink noise; homogeneous sample.

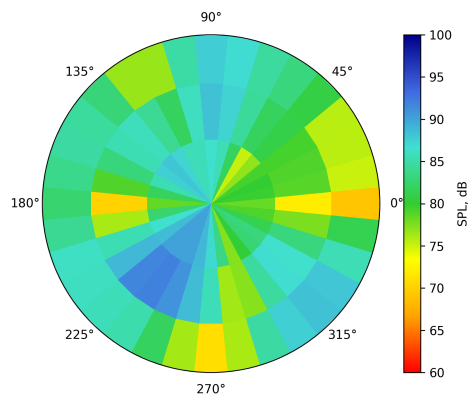


FIG. 8. Sound pressure level (200 Hz) in the source room, source position no. 1, sine wave; homogeneous sample.

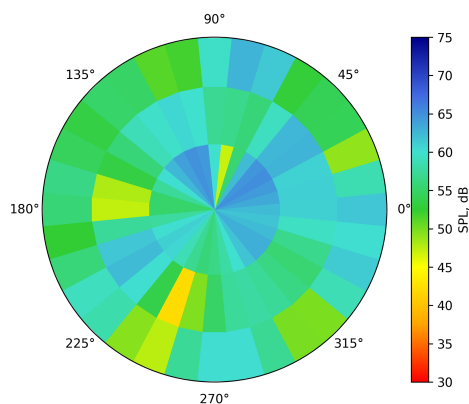


FIG. 9. Sound pressure level (200 Hz) in the receiving room, source position no. 1, sine wave; homogeneous sample.

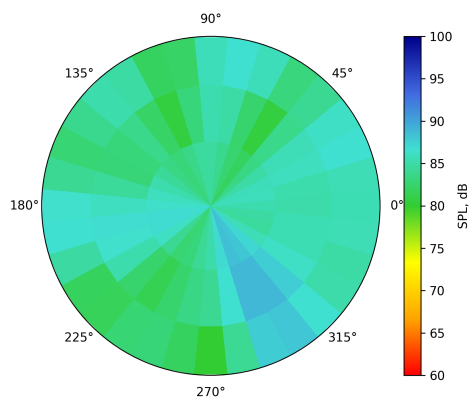


FIG. 10. Sound pressure level (200 Hz) in the source room, source position no. 1, FM sine wave; homogeneous sample.

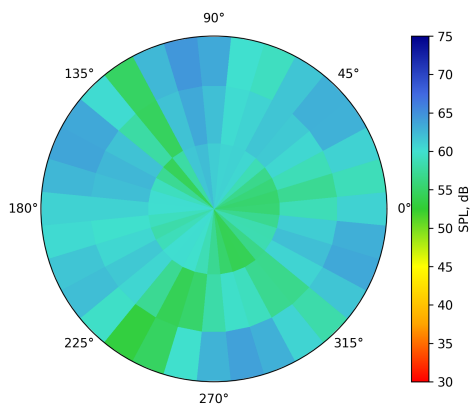


FIG. 11. Sound pressure level (200 Hz) in the receiving room, source position no. 1, FM sine wave; homogeneous sample.

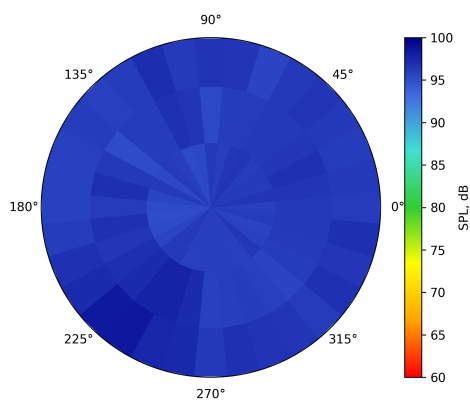


FIG. 12. Sound pressure level (500 Hz) in the source room, source position no. 2, pink noise; two-layer sample.

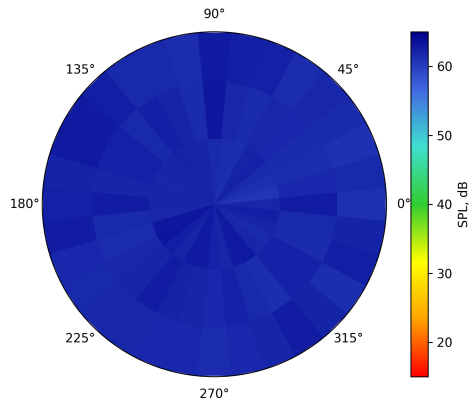


FIG. 13. Sound pressure level (500 Hz) in the receiving room, source position no. 2, pink noise; two-layer sample.

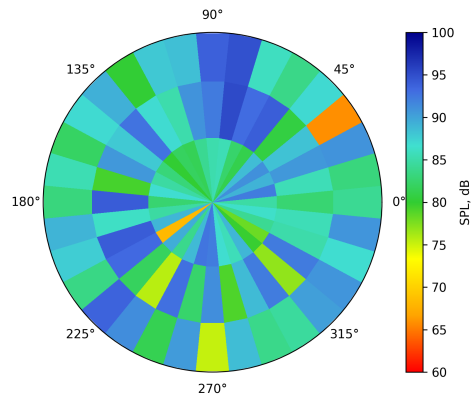


FIG. 14. Sound pressure level (500 Hz) in the source room, source position no. 2, sine wave; two-layer sample.

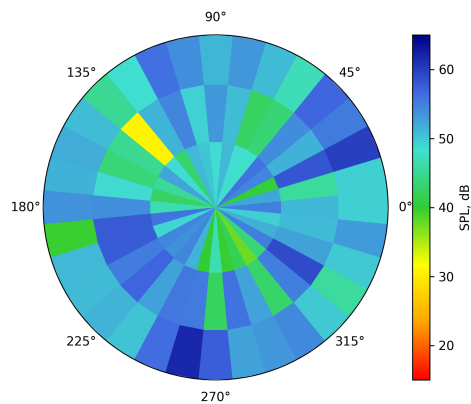


FIG. 15. Sound pressure level (500 Hz) in the receiving room, source position no. 2, sine wave; two-layer sample.

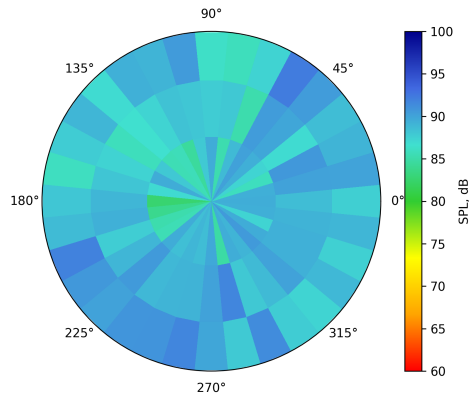


FIG. 16. Sound pressure level (500 Hz) in the source room, source position no. 2, FM sine wave; two-layer sample.

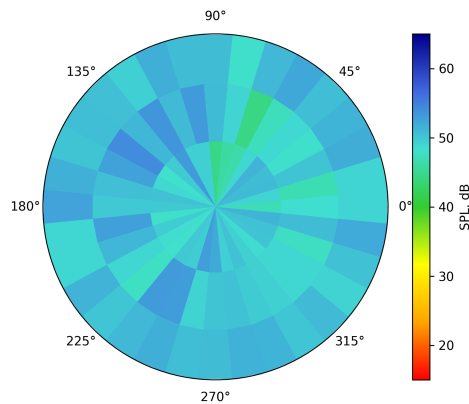


FIG. 17. Sound pressure level (500 Hz) in the receiving room, source position no. 2, FM sine wave; two-layer sample.

these cases are not included. However, all measurement sessions were thoroughly considered in the subsequent numerical calculations, which included a detailed assessment of the overall dispersion observed in the results.

3.3. Sound insulation

The sound insulation measurement in third-octave bands across the full frequency range from 50 Hz to 5 kHz was performed using pink noise, and the results for the homogeneous sample are presented in Fig. 18. In further analysis, this result was used as a reference measurement for the comparative evaluation of the results obtained with tonal excitation and FM signals. The data dispersion is indicated by dashed lines as error bars on the graph, providing a visual representation of the variability in the measurement.

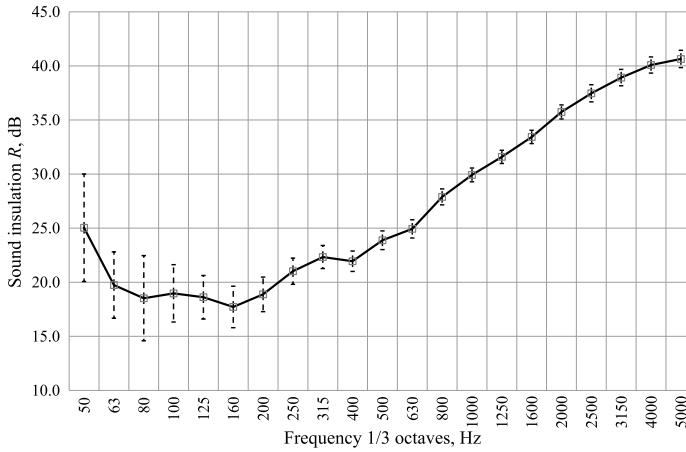


FIG. 18. Sound insulation of homogenous sample measured using broadband noise.

The average values of acoustic insulation for each sample were calculated (Tables 5 and 6) according to Eq. (2.1), and the combined standard uncertainty $u_c(R)$ and expanded uncertainty $U_{95}(R)$ were determined in accordance with the assumptions presented in Subsec. 2.5. In the final row (Tables 5 and 6), the mean value was calculated to facilitate a single-number comparison of the obtained values.

TABLE 5. Sound insulation of homogenous sample.

Type of excitation	Pink noise			Sine wave			FM sine wave		
	Average, dB	$u_c(R)$, dB	$U_{95}(R)$, dB	Average, dB	$u_c(R)$, dB	$U_{95}(R)$, dB	Average, dB	$u_c(R)$, dB	$U_{95}(R)$, dB
100 Hz	19.0	2.7	5.3	30.2	8.5	17.0	27.2	5.7	11.5
200 Hz	18.9	1.6	3.2	20.8	8.6	17.2	17.5	3.9	7.8
315 Hz	22.3	1.1	2.1	22.2	8.7	17.3	24.3	3.3	6.7
500 Hz	23.9	0.9	1.7	22.7	9.5	19.0	19.4	2.6	5.1
Average (100–500 Hz)	21.0	1.5	3.1	24.0	8.8	17.6	22.1	3.9	7.8
Average (200–500 Hz)	21.7	1.2	2.4	21.9	8.9	17.8	20.4	3.3	6.6

The variation in the average sound insulation values in third-octave bands depending on the applied excitation signal is shown in Fig. 19. The results presented in figure below facilitate the observation of the impact of excitation

TABLE 6. Sound insulation of two-layer sample.

Type of excitation	Pink noise			Sine wave			FM sine wave		
Results	Average, dB	$u_c(R)$, dB	$U_{95}(R)$, dB	Average, dB	$u_c(R)$, dB	$U_{95}(R)$, dB	Average, dB	$u_c(R)$, dB	$U_{95}(R)$, dB
100 Hz	22.3	3.0	6.0	33.8	8.5	17.0	32.4	6.2	12.4
200 Hz	20.4	1.8	3.7	18.3	12.5	24.9	21.5	3.9	7.8
315 Hz	24.3	1.6	3.1	22.9	11.4	22.7	22.4	4.4	8.7
500 Hz	25.7	2.1	4.2	26.8	8.7	17.4	24.0	2.4	4.7
Average (100–500 Hz)	23.2	2.1	4.2	25.4	10.3	20.5	25.1	4.2	8.4
Average (200–500 Hz)	23.5	1.8	3.7	22.7	10.8	21.7	22.6	3.5	7.1

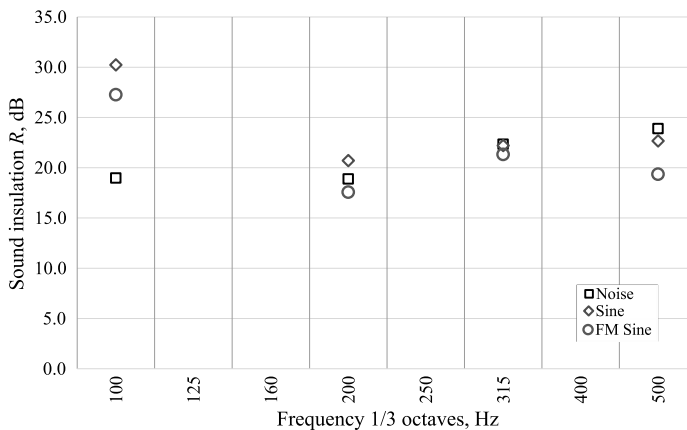


FIG. 19. Sound insulation of homogenous sample using different excitations.

type (tonal excitation modulated and noise excitation) on the sound insulation results measured in 1/3 octave bands. With tonal excitation, the highest insulation value was obtained at the 100 Hz frequency band (Fig. 19). This band also exhibited the most significant data dispersion (Fig. 20). The expanded uncertainty was 5.3 dB with noise excitation, 17.0 dB with tonal excitation, and 11.5 dB with FM excitation (Table 5). In the other analyzed third-octave bands, the results are more closely aligned. When using FM excitation, the results fall “between” those obtained with noise and tonal excitation, though with a slightly larger deviation in the 500 Hz band.

Employing tonal excitation, the highest value of sound insulation was obtained in the 100 Hz frequency band, which also exhibited the widest variability of measurements across all examined third-octave bands (Fig. 19), ranging from 8.5 dB to 9.5 dB.

Conversely, the findings acquired using FM excitation show intermediate values of sound insulation, with decreasing dispersion at higher frequencies (Fig. 21).

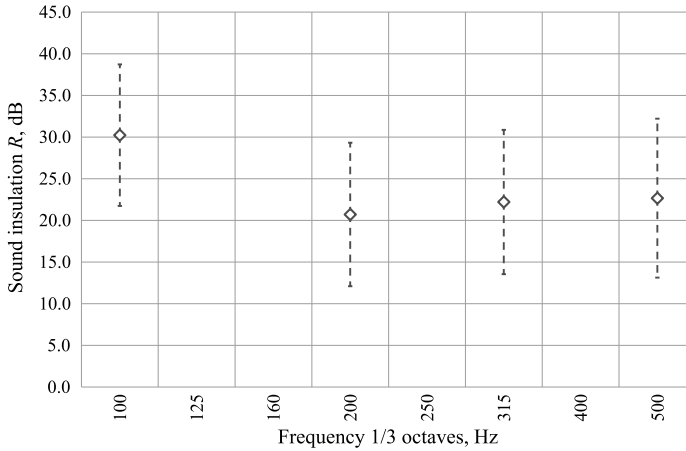


FIG. 20. Sound insulation of homogenous sample using tonal excitation.

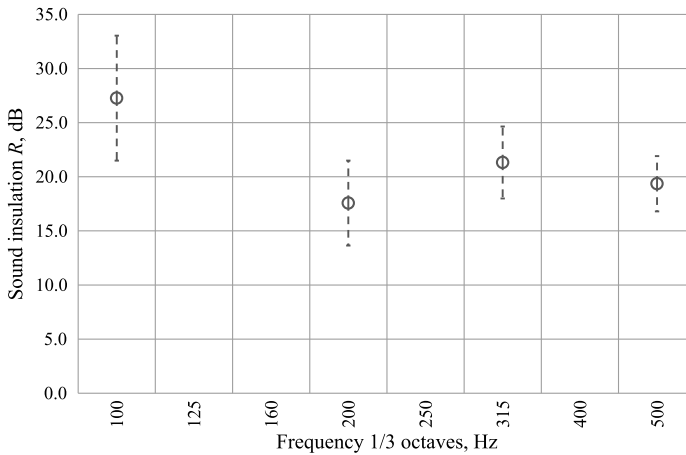


FIG. 21. Sound insulation of homogenous sample using FM excitation.

The results of the sound insulation calculations for the layered sample are presented in Table 6. Based on the results in Table 6, it can be observed that the type of excitation significantly impacts both the acoustic insulation and the measurement uncertainty.

The results presented in the figure below illustrate the impact of excitation type (tonal, modulated and noise excitation) on sound insulation measurements in 1/3 octaves bands. The highest value of sound insulation was obtained using tonal excitation, with an average value across all analyzed third-octave bands of 25.4 dB. This value is heavily influenced by an outlier result in the 100 Hz band, where insulation reached 33.8 dB, which is significantly higher than the results obtained with other excitations. The lowest acoustic insulation was measured with pink noise excitation, with an average value of 23.2 dB, showing a noticeable increase in insulation at higher frequencies (25.7 dB at 500 Hz). The results obtained with FM excitation were similar to those with tonal excitation, but with less dispersion. Both the standard and expanded uncertainties were lower. Comparing the averaged values of expanded uncertainty to that determined with pink noise (4.2 dB), tonal excitation resulted in a five-fold increase (20.5 dB), while FM excitation yielded a two-fold increase (8.4 dB). Additionally, the sound insulation of the layered sample was measured (Fig. 22) using pink noise across third-octave bands in the frequency range of 50 Hz to 5 kHz.

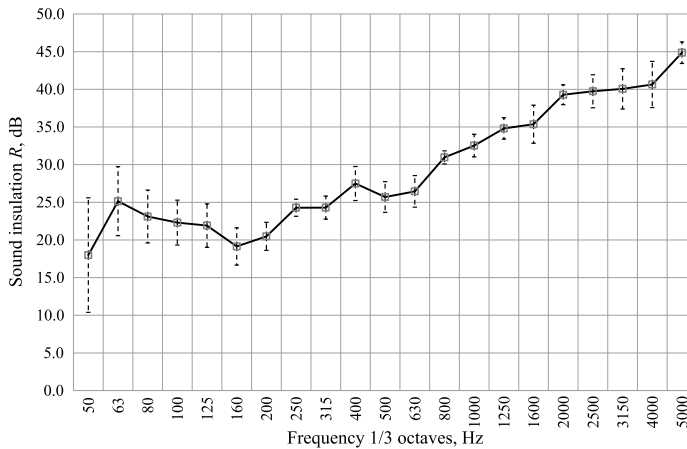


FIG. 22. Sound insulation of layered sample measured using broadband noise.

Comparing the average acoustic insulation values of the layered sample, it is also difficult to observe a clear trend indicating a dependence of insulation on the type of excitation. In the 200 Hz, 315 Hz, and 500 Hz third-octave bands, the results are similar, without any noticeable trend (Fig. 23). However, in the 100 Hz band, both tonal and FM excitations yielded significantly higher insulation values compared to pink noise excitation.

The result variations for tonal excitation are shown in Fig. 24, while those for FM tonal excitation are depicted in Fig. 25. As with the plexiglass sample,

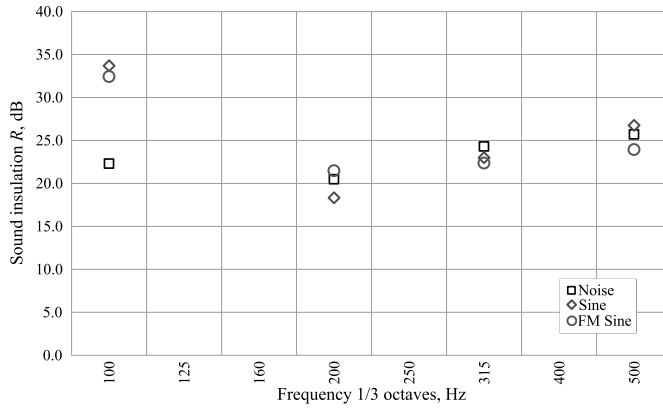


FIG. 23. Sound insulation of layered sample using different excitations.

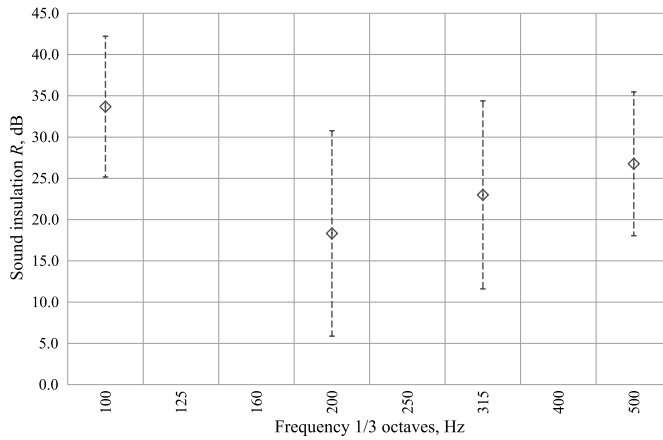


FIG. 24. Sound insulation of layered sample using tonal excitation.

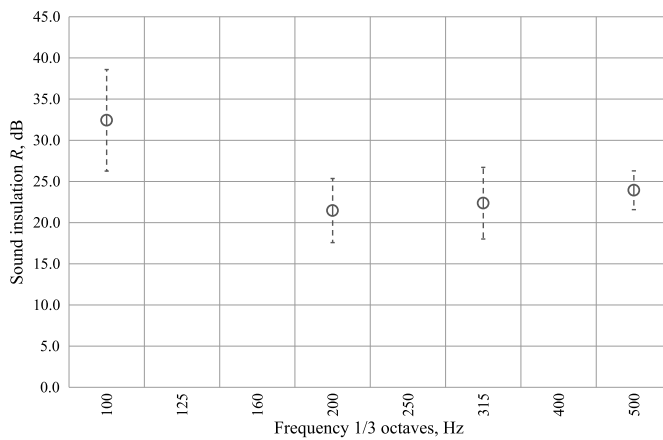


FIG. 25. Sound insulation of layered sample using FM excitation.

the result variations are significantly larger with tonal excitation compared to FM tonal excitation, without any substantial difference in the obtained sound insulation values.

The results obtained with FM excitation demonstrate intermediate values of sound insulation, with the degree of variation diminishing at higher frequencies (Fig. 25). The highest dispersion, measuring 6.2 dB, is observed in the lowest band of 100 Hz, while the smallest variation of 2.4 dB, is found in the 500 Hz band. Variations for the 200 Hz and 315 Hz bands exhibit comparable levels, measuring 3.9 dB and 4.4 dB, respectively.

4. SUMMARY AND CONCLUSIONS

This study aimed to assess airborne sound insulation by employing tonal excitation. However, due to considerable variations in the sound pressure level distribution across both testing chambers, additional measurements were conducted utilizing FM tonal excitation. The resulting data were then compared with measurements obtained under tonal and broadband noise-based stimuli. The comparative analysis focused on the acoustic insulation measurement outcomes, as well as the variability in the determined values of L_1 , L_2 , and T . For each sample tested, the L_1 , L_2 , and T values were derived from measurements taken at 192 distinct locations.

The noise excitation measurements across the full frequency spectrum were used as a benchmark. Tonal and FM excitation measurements were performed at 100 Hz, 200 Hz, 300 Hz, and 500 Hz, corresponding to the 1/3 octave band center frequencies of 100 Hz, 200 Hz, 315 Hz, and 500 Hz. The evaluation of the method was based on the variations in sound pressure levels in the source room, receiving room, and reverberation time in the receiving room. The tests were carried out on two distinct samples placed in the measurement aperture of the reverberation chamber located at the Department of Mechanics and Vibroacoustics at AGH University of Science and Technology in Krakow.

The research findings can be summarized as follows:

- Tonal excitation yielded the highest variability in sound insulation and uncertainty results across most frequency bands, whereas noise excitation produced the lowest variations. For both samples, the expanded uncertainty calculated from average value (100–500 Hz) was five times greater: 17.6 dB to 3.1 dB for the homogenous sample and 20.5 dB to 4.2 dB for the two-layer sample. Similarly, for the average calculated in 200–500 Hz, the expanded uncertainty was again about five times larger for tonal excitation: 17.8 dB to 2.4 dB for the homogenous sample and 21.7 dB to 3.7 dB for the two-layer sample, compared to pink noise excitation.

- The values of the measured sound insulation in the 200, 315, and 500 Hz bands were similar regardless of the excitation type, with no noticeable trend.
- At the 100 Hz band, significantly higher results of sound insulation were obtained with tonal and FM excitations compared to noise excitation. For the homogeneous sample, values were 30.2 dB and 27.2 dB for tonal and FM excitations, respectively compared to 19 dB for noise excitation, representing a difference of 11.2 dB and 8.2 dB. For the two-layer sample, values were 33.8 dB (sine) and 32.4 dB (modulated sine) compared to 22.3 dB for noise excitation, with differences of 11.5 dB and 10.1 dB, respectively.
- Despite the overall high measurement uncertainty in the 100 Hz band, along with the relatively consistent of results in the other frequency bands and the significantly lower variation (approx. 10 dB smaller expanded uncertainty both in individual and averaged values) with FM excitation compared to tonal excitation, it can be concluded that the introduction of FM improved the quality of the measurement results relative to tonal excitation.
- In cases with fewer measurement points, which is standard even for high-accuracy measurements, it is expected that the average values of sound insulation will differ more depending on the type of excitation used, corresponding to the standard uncertainty.

ACKNOWLEDGMENTS

This research was financed by research subsidy no. 16.16.130.942/kmiw, held in Department of Mechanics and Vibroacoustics at the Faculty of Mechanics and Robotics at AGH University of Krakow, Poland. The authors declare no known competing financial interests or personal relationships that could have influenced the work reported in this paper.

REFERENCES

1. ISO 10140-4, *Acoustics – Laboratory measurement of sound insulation of building elements – Part 4: Measurement procedures and requirements*, 2021.
2. HAK C.C., VAN HOUT N.H., MARTIN H.J., Measuring sound insulation using deconvolution techniques, *The Journal of the Acoustical Society of America*, **123**(5_Supplement): 3501–3501, 2008, <https://doi.org/10.1121/1.2934378>.
3. HUNT F.V., On frequency modulated signals in reverberation measurements, *The Journal of the Acoustical Society of America*, **5**(2): 127–138, 1933, <https://doi.org/10.1121/1.1915640>.

4. COOK R.K., Modulated reverberation – a new method for measurement of absorption and sound power, *The Journal of the Acoustical Society of America*, **54**(1_Supplement): 302, 1973, <https://doi.org/10.1121/1.1978180>.
5. OZIMEK E., RUTKOWSKI L., Deformation of frequency modulated (FM) signals propagating in a room, *Applied Acoustics*, **26**(3): 217–230, 1989, [https://doi.org/10.1016/0003-682X\(89\)90055-8](https://doi.org/10.1016/0003-682X(89)90055-8).
6. JCGM 100: 2008, *Evaluation of measurement data – Guide to the expression of uncertainty in measurement*, 2008.
7. WSZOLEK T., Uncertainty of sound insulation measurement in laboratory, *Archives of Acoustics*, **32**(4S): 271–277, 2007.

Received August 11, 2024; accepted version December 17, 2024.

Online first January 21, 2025.
